

Chapter 1

Energy loss

1.1 Introduction

In gas-based detectors, particle trajectories are measured using the ionisation electrons that are generated by the particle. Garfield is currently interfaced with two programs that simulate the ionisation process: Heed for high-energy charged particles and photons, and SRIM which caters for low-energy ions.

1.2 Available models

1.2.1 Heed

The Heed program [Igor Smirnov, NIM A 554 (2005) 474] is designed to simulate the ionisation patterns created by charge ± 1 hadrons traversing a nearly arbitrary gas mixture. An underlying assumption is that the hadrons lose only a small part of their energy in the process. Heed can also process the absorption of low-energy ($\epsilon < 10$ keV) photons. Heed is not designed to simulate heavily ionising particles, such as ions, which stop in the gas.

The part of the program that computes the energy transfer from a charged particle to the gas molecules is based on the PAI model. Heed goes much further than this model and has built-in knowledge of the electron energy levels inside the gas molecules which it uses to generate (and re-absorb) fluorescence photons from excited states. Heed also incorporates a detailed model for the transformation of the energy transferred to the gas into spatial ionisation patterns, with the appropriate fluctuations.

Heed has been tested extensively and is widely used by high-energy physics experiments.

1.2.2 SRIM

The SRIM program [www.srim.org] deals with ions which stop in a material. The output of the program contains tables of the mean electromagnetic and hadronic differential energy loss, the transverse and longitudinal straggling, and the range, all as function of the energy of the

ion. Fig. 1.1 shows two examples of such data. SRIM unfortunately does not provide statistical information other than these averages, and the distribution parameters have therefore to be taken from other sources. These models are described in the remainder of this chapter.

A companion program, TRIM, does generate individual events. Sadly however, this program does not seem to be available in source form for interfacing.

1.3 Mean energy loss

From the SRIM differential energy loss tables, one can compute the mean energy loss over a step of any length by integrating

$$\epsilon'(x) = -\frac{dE}{dx}(\epsilon(x))^{\text{em}} - \frac{dE}{dx}(\epsilon(x))^{\text{hd}},$$

where $\epsilon(x)$ is the energy of the ion at a point x . This differential equation can be solved analytically in a number of simple cases, e.g. for a linear dependence of the differential energy loss on the energy of the particle, in which case the energy of the particle will fall exponentially. Given that the solution will in general be non-linear, caution needs to be exercised when integrating the energy loss over steps of any length. Garfield uses a comparison of Runge-Kutta methods to control the sub-step size.

1.4 Electromagnetic energy loss fluctuations

1.4.1 Introduction

A broad range of models to describe electromagnetic energy loss fluctuation, sometimes called straggling, has been developed. Popular versions involve Landau, Vavilov, Gaussian and other functions, as well as combinations of these. None of these models is particularly accurate, and it is therefore not meaningful to argue about the subtleties of the shapes of these distributions, as pointed out in the review by Hans Bichsel [Reviews of Modern Physics, Volume 60, July 1988, p663-699].

1.4.2 Notation

In the following, we will give expressions for the distribution of the energy ϵ that is lost by a particle with mass m_p , kinetic energy E_{kin} , velocity

$$\beta = \frac{v}{c} = 1 - \frac{1}{(1 + E_{\text{kin}}/m_p)^2},$$

matching γ and charge z , while traversing a layer of material of thickness d , density ρ , atomic weight A and atomic number Z . We write $\bar{\epsilon} = d \, dE/dx$ for the mean energy loss. The energy

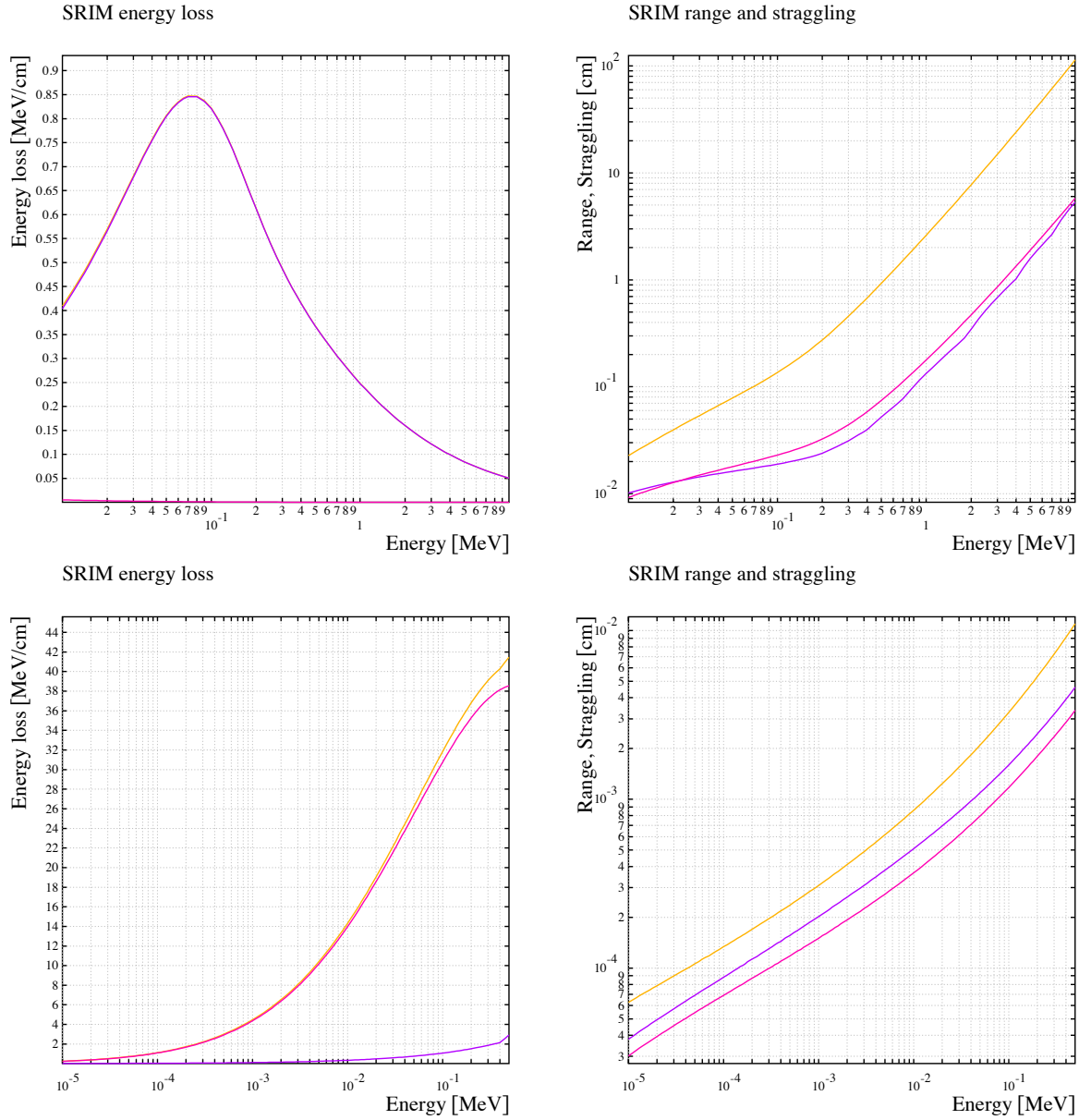


Figure 1.1: The differential energy loss and straggling as computed by SRIM for an H^+ ion in Ar (top row) and a Pb^+ ion in Xe (bottom row). In the differential energy loss graphs, orange lines represent total differential energy loss, purple lines the electromagnetic components and pink lines the hadronic component. In the straggling graphs, the orange lines show the total range, the purple lines the longitudinal straggling and the pink lines the transverse straggling. H^+ ion in Ar serves as an example in the rest of this chapter since it can be treated both by SRIM and by Heed. Energy loss is almost entirely electromagnetic in this case, which is in marked contrast with Pb^+ ion in Xe where hadronic energy loss dominates.

loss term dE/dx , which depends on the kinetic energy of the particle, needs to be provided independently, e.g. by the SRIM program. An energy loss parameter ξ is assumed to be given by

$$\xi = 0.153... \frac{z^2 Z}{\beta^2 A} \rho d.$$

For the maximum energy which can be transferred in in any one collision, we use the expression

$$E_{\max} = \frac{2m_e \beta^2 \gamma^2}{1 + 2\gamma m_e/m_p + (m_e/m_p)^2},$$

where m_e is the electron mass. The ratio κ of ξ and E_{\max} is one of the key parameters when deciding which generator to use:

$$\kappa = \xi/E_{\max}.$$

Bear in mind that κ is proportional to the step size d .

1.4.3 Landau distribution

Applicability

The Landau distribution is designed to describe the energy loss in layers of material where the mean energy loss is small compared to the largest energy which can be transferred in any single collision. This typically applies when the absorbing layers are thin. In addition, for the Landau approximation to be valid, the layer must be sufficiently thick for ξ to be large compared with the ionisation potential of the material that is traversed. In the example used here, gaseous argon, the relevant ionisation potential is 15.7 eV and the Landau approximation is accordingly expected to be fail for $d < 10 - 100 \mu\text{m}$.

Sampling parameter

When applying the Landau distribution, we do not sample $f_L(\lambda)$ at

$$\lambda = \frac{\epsilon - \bar{\epsilon}}{\xi}$$

as one might expect, but rather at

$$\lambda = \frac{\epsilon - \bar{\epsilon}}{\xi} - 1 + \gamma_E - \beta^2 - \log\left(\frac{\xi}{E_{\max}}\right),$$

where $\gamma_E \approx 0.5772$. The reason for doing so is twofold: this ensures that the convolution properties (Sect. 1.3.7) are satisfied and this provides continuity between the Landau, Vavilov and Gaussian distributions.

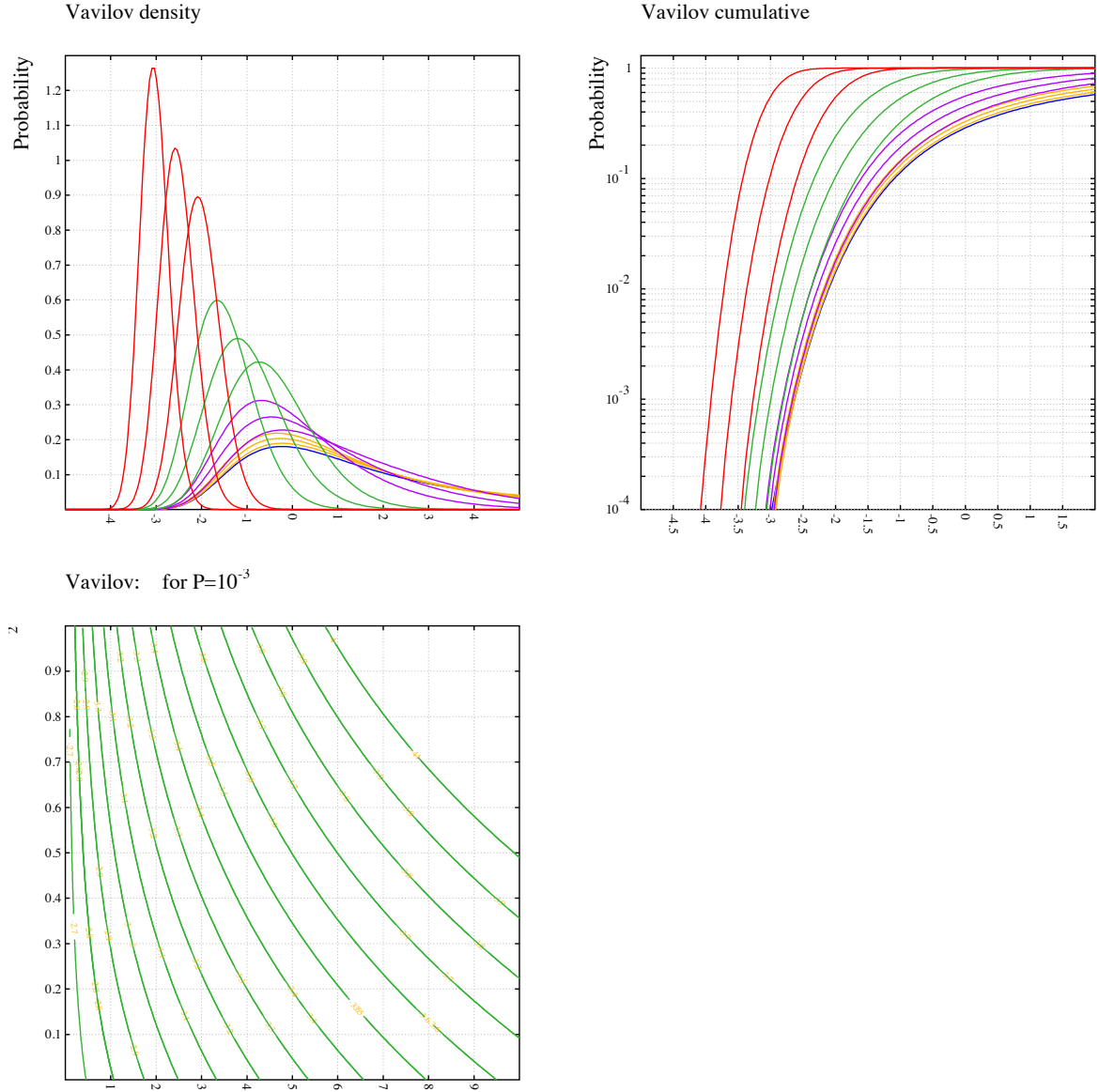


Figure 1.2: The Landau and Vavilov distributions. Blue: Landau. Orange, purple, green and red: Vavilov distributions for κ ranging from 0.05 (orange) to 5 (red) and β^2 from 0 (peaking on the right) to 1 (peaking on the left). The contours of the lower graph show the sampling parameter λ value below which the cumulative probability is 10^{-3} .

Undefined mean

A technical problem with the Landau distribution $f_L(\lambda)$ is that it doesn't have a mean in the sense that

$$\int_{-\infty}^{\lambda_{\max}} \lambda f_L(\lambda) d\lambda \rightarrow \infty$$

as $\lambda_{\max} \rightarrow \infty$. This is a consequence of the slowly decaying high- λ tail of the Landau distribution, which in itself is normalised:

$$\int_{-\infty}^{\infty} f_L(\lambda) d\lambda = 1.$$

Not having a definite mean is not a problem as long as we are dealing with analytic expressions for the energy loss distribution, but this leads to large and unphysical fluctuations when generating Monte Carlo events since occasionally energy losses will exceed the kinematic maximum. In order to have a definite mean, the conventional solution consists in imposing $\lambda < \lambda_{\max}$ such that the mean $\bar{\lambda}$ of the truncated distribution has the desired value. The relation between $\bar{\lambda}$ and λ_{\max} can be approximated by

$$\bar{\lambda} = (p_0 + p_1 \lambda_{\max} + p_2 \lambda_{\max}^2 + p_3 \lambda_{\max}^3) + (p_4 + p_5 \lambda_{\max}) e^{p_6 \lambda_{\max}}$$

with coefficients p_i computed by numeric integration. This approach hardly has a physics basis, but given the overall accuracy we expect from this model, this should not be a point of major concern.

When applying the Landau distribution, we truncate the Landau distribution such that the mean has the value

$$\bar{\lambda} = -1 + \gamma_E - \beta^2 + \log\left(\frac{\xi}{E_{\max}}\right)$$

which gives the mean of ϵ the desired value, $\bar{\epsilon}$.

Negative energy loss

By eliminating high energy loss fluctuations, we have ensured that the mean energy loss as generated with the Landau distribution has the desired value. Unfortunately, as we will see below, this correct value of the mean is obtained in part through negative energy loss values. Negative energy losses are, of course, not physical and they must be avoided. Contrary to the situation at high energies, truncation at zero energy is not an option since such a truncation grossly distorts the distribution in a domain where it is deemed most accurate.

The Landau distribution $f_L(\lambda)$ decays exponentially towards negative λ : there is a 10^{-4} probability to find a $\lambda < -3$ and the distribution is numerically zero for $\lambda < -5$, see Fig. 1.2. Assuming we are willing to accept the 10^{-3} risk of generating a negative energy loss, then we have to require

$$\frac{\bar{\epsilon}}{\xi} + \beta^2 + \log \kappa > 2 + \gamma_E.$$

This condition is difficult to satisfy for thin layers, a priori the domain where one applies the Landau distribution. We consider the Landau distribution for $\kappa < 0.05$ ($\log \kappa < -3$) while conventionally, the Landau distribution is applied only for $\kappa < 0.01$ ($\log \kappa < -4.6$).

In the example of Fig. 1.6, where $\beta^2 \approx 0.002$, the condition imposes a step size $d > 54 \mu\text{m}$ or a $\kappa > 0.14$, i.e. there is for $E_{\text{kin}} = 1 \text{ MeV}$ protons in Ar no regime where the Landau distribution can be used without generating negative energy losses. This is can also be seen from the Landau case in the figure: the step size $d = 10 \mu\text{m}$ is such that $\kappa = 0.026$, and the cut-off at zero energy is clearly visible.

The approach adopted in the combined energy loss fluctuation model described in Sect. 1.3.6 consists in switching, if possible, to larger steps, thereby entering the domain where the Vavilov and Gaussian distributions become applicable. A warning is issued should no such increase in step size be possible, for instance because the smallest acceptable step size exceeds the distance that remains to be traversed.

1.4.4 Vavilov distribution

Applicability

The Vavilov distribution is a variation on the Landau distribution which is intended to be a better approximation in case the mean energy loss is approaching the largest energy which can be transferred in any single collision. To this effect, the distribution depends on the parameter $\kappa = \xi/E_{\text{max}}$. The distribution also depends on β^2 . For small κ and large β^2 , the Landau and Vavilov distribution are very similar.

Sampling parameter

The Vavilov distribution is allegedly meant to be sampled at

$$\lambda = \kappa \left(\frac{\epsilon - \bar{\epsilon}}{\xi} - 1 + \gamma_E - \beta^2 \right).$$

Using this sampling parameter does not (at all) lead to a smooth transition of the energy loss distribution between the regimes covered by the Vavilov and Landau distributions. Given that the Vavilov distribution function at small κ is virtually identical to the Landau distribution, we sample the Vavilov distribution with the same parameter as the Landau distribution.

Mean

Contrary to the Landau distribution, the Vavilov distribution has a defined mean for all (κ, β^2) . Truncations at high energy therefore do not have to be applied. Moreover, the mean of this distribution is such that, with the above sampling parameter, the mean energy is indeed $\bar{\epsilon}$, as shown in Fig. 1.3.

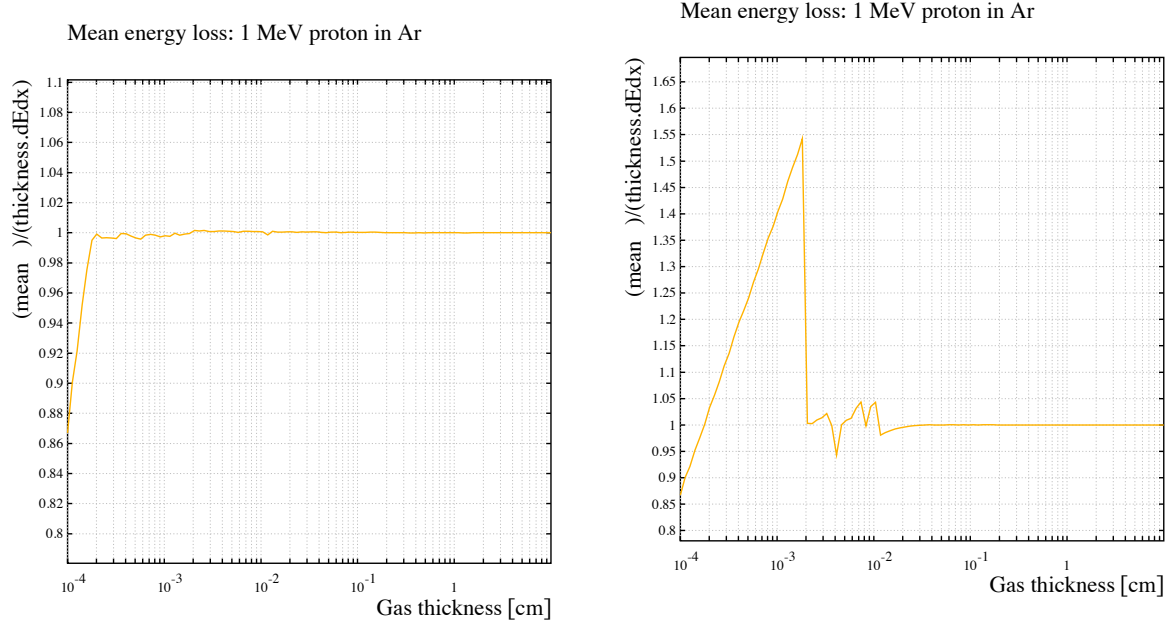


Figure 1.3: The mean energy loss should equal $d \, dE/dx$, as verified here for a proton with kinetic energy $E_{\text{kin}} = 1 \text{ MeV}$ in Ar gas, and a step size d ranging from $2 \text{ } \mu\text{m}$ to 10 cm . On the left, a truncated Landau distribution has been used for $d < 20 \text{ } \mu\text{m}$, a high-precision Vavilov distribution for $20 \text{ } \mu\text{m} < d < 1.7 \text{ mm}$ and a Gaussian distribution for $1.7 \text{ mm} < d$. Negative energies have not been removed. On the right, a regular Landau distribution and a fast Vavilov distribution have been used. The fast Vavilov generator leads in this case to a 5 % error. For $d < 2 \text{ } \mu\text{m}$, the truncation of the Landau distribution ceases to have an effect.

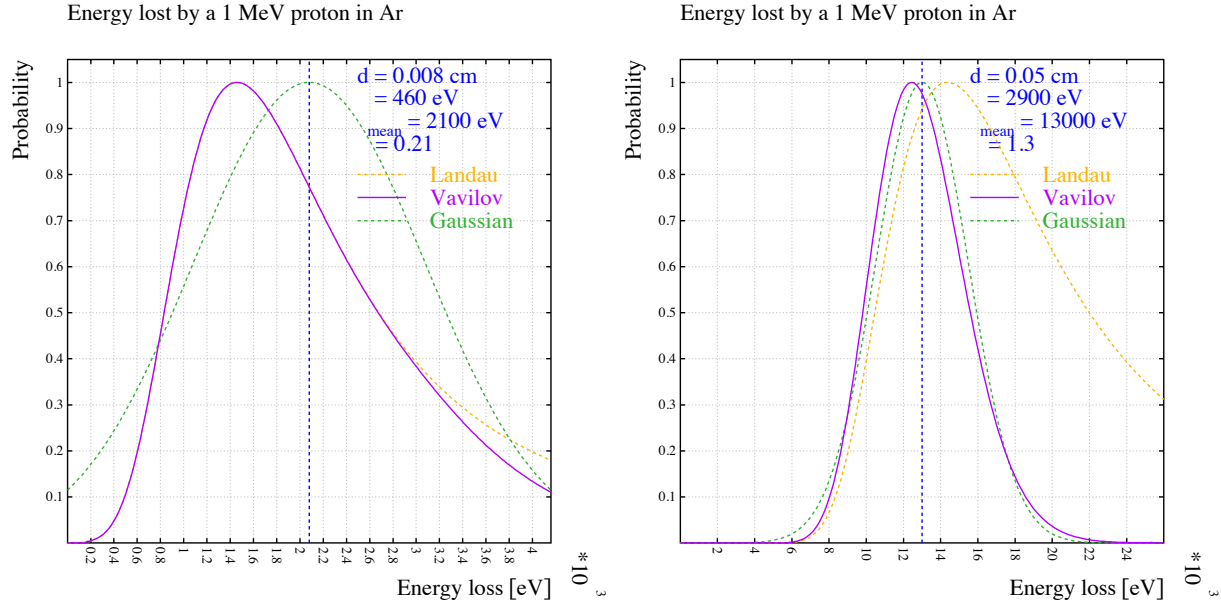


Figure 1.4: Transitions between the Landau and Vavilov distributions (left) and between the Vavilov and Gaussian distributions (right). For the colour coding, see Fig. 1.6.

Negative energy loss

Like the Landau distribution, the Vavilov distribution potentially leads to negative energy losses. The conditions for this to happen are the similar to those for the Landau distribution, except that there is a (κ, β^2) dependence, as can be seen from Fig. 1.2, which prompts the use of an adjustable threshold: $\lambda > -2.7$ for $\kappa < 0.1$, $\lambda > -3.2$ for $0.1 < \kappa < 1$ and $\lambda > -4$ for $1 < \kappa < 5$.

As with the Landau distribution, the approach to deal with negative energy losses is to increase the step size until this risk vanishes. A warning is issued should no such increase in step size be possible, for instance because the smallest acceptable step size exceeds the distance that remains to be traversed.

Generators

Vavilov random numbers are expensive to generate if a high level of precision is required. The main reason for this is the non-trivial dependence of the function on its parameters κ and β^2 . The CERN program library provides a generator which is fast, but only accurate to 2 decimal places, but also provides high-precision distribution function. The Garfield interface offers the choice between the fast and inaccurate generator, and a much slower generator based on the high-precision distribution function. The importance of this choice can be judged from Fig. 1.3.

1.4.5 Gaussian distribution

Applicability

For large κ , and using the Landau sampling parameter, the Vavilov distribution is almost Gaussian with a mean equal to $\bar{\epsilon}$ and a width equal to

$$\sigma^2 = \xi E_{\max} \left(1 - \frac{1}{2}\beta^2\right).$$

Note that σ^2 is proportional to the step size d through the ξ term, a property which will be used when checking the convolution properties in Sect. 1.3.7.

Negative energy loss

Whilst not an issue for a proton traversing argon, negative energy losses in the Gaussian regime can easily occur for slow, heavy ions. It is almost always the Gaussian regime that applies for such ions since their β^2 is small, which makes their maximum energy transfer E_{\max} small and their ξ large, as a result of which κ becomes large.

Such particles lose their energy fast, but they do so essentially through nuclear interactions, as shown in Fig. 1.1 for a Pb^+ ion in Xe.

Let us consider a Pb^+ with a kinetic energy $E_{\text{kin}} = 100$ keV traversing Xe, illustrated in Fig. 1.5. According to SRIM, such a Pb^+ stops after $32 \mu\text{m}$. One is therefore tempted to simulate this process on the scale of microns.

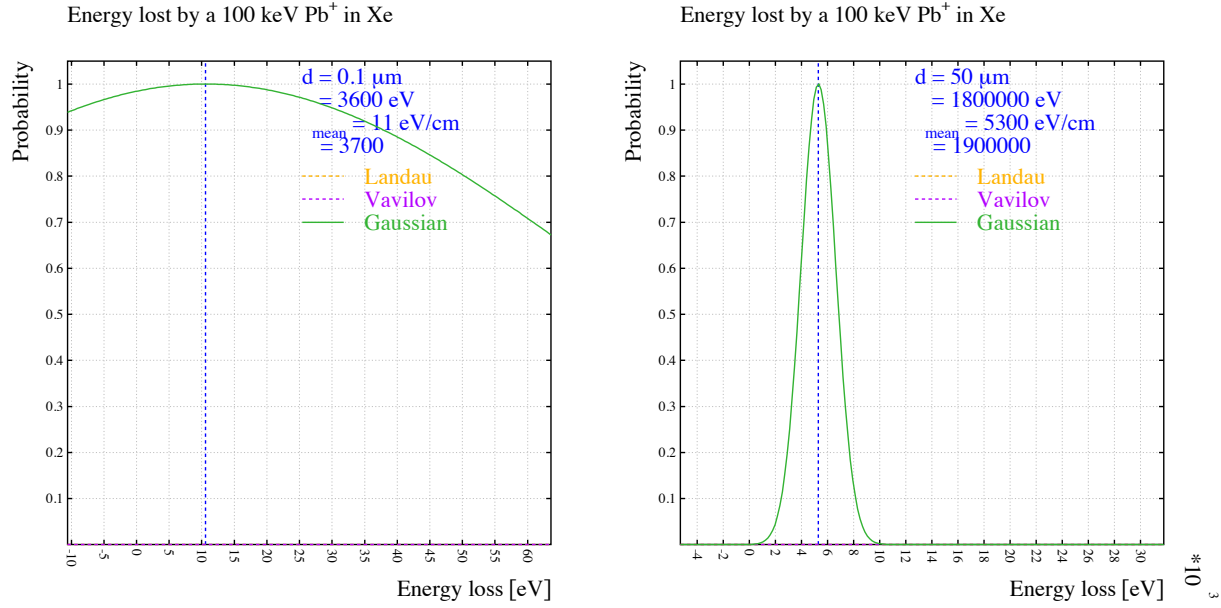


Figure 1.5: The distributions of the energy loss for a Pb^+ ion proton with a kinetic energy of $E_{\text{kin}} = 100 \text{ keV}$ in Xe layers of thickness $d = 0.1 \mu\text{m}$ and $d = 50 \mu\text{m}$ as computed with SRIM and applying Gaussian fluctuations as described in the text. Note the substantial probability of having negative energy losses for the $d = 0.1 \mu\text{m}$ layer.

The differential electromagnetic energy loss of a proton in Ar is of the same order of magnitude as that of a Pb^+ ion in Xe. Also the product ξE_{max} , which determines the width, has, for equally thick layers of gas, comparable values for the two configurations. The major difference resides in the gas thickness d : mm to cm for a proton in Ar and sub-micron for a Pb^+ ion in Xe. At the vastly larger natural scale of a proton in Ar, the ratio of width over mean, which scales with $1/\sqrt{d}$, is far more favourable than it is for a Pb^+ ion in Xe.

As with the Landau and Vavilov distributions, we avoid negative energy loss by increasing the step size. Should the remaining distance to be travelled be smaller than the minimum step size which avoids negative energy losses, then no energy losses are applied to the step and a warning is issued.

1.4.6 Combined model

Approach

Given that none of the three above models is expected to be appropriate for all κ , the most promising approach is to combine them as follows:

- $\kappa < 0.05$: Landau distribution;
- $0.05 < \kappa < 5$: Vavilov distribution;

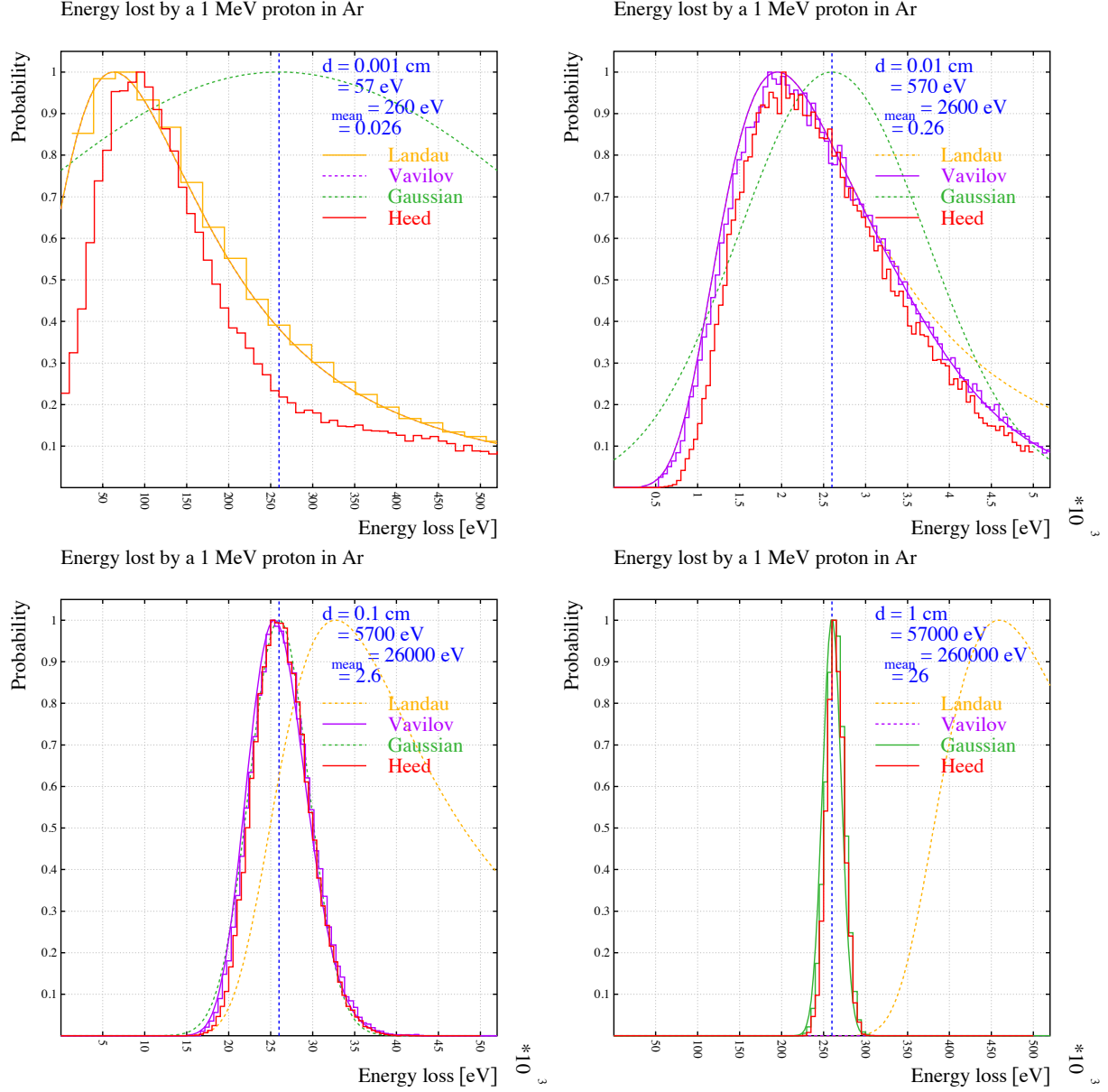


Figure 1.6: The distributions of the energy loss for a proton with a kinetic energy of $E_{\text{kin}} = 1$ MeV in layers of $10 \mu\text{m}$, $100 \mu\text{m}$, 1 mm and 1 cm of Ar as computed with SRIM and fluctuated using the models described in the text, agree to a reasonable extent with the Heed calculations (red histograms). The Landau distribution (orange) has been used for $d = 10 \mu\text{m}$, the Vavilov distribution (purple) for $d = 100 \mu\text{m}$ and $d = 1$ mm, and the Gaussian distribution (green) for $d = 1$ cm. Solid lines of a given colour show the distribution function of the applicable model, histograms show distributions generated for the applicable model and dashed lines show inapplicable models. Note that the Gaussian model fails badly for the thinnest layers while the Landau distribution fails for the thicker layers.

- $5 < \kappa$: Gaussian distribution.

In combining these distributions, we want to ensure that the following requirements are satisfied:

- the distribution truly has the desired mean;
- no negative energy losses occur;
- no abrupt changes when moving from one model to another;
- plausible results.

Stability of the mean

As shown in Fig. 1.3, the mean energy as generated by these three distributions does indeed assume the correct value, except for very thin layers.

It is also apparent from the figure that the truncation of the Landau distribution is instrumental in ensuring that the mean is stable. Using the high-precision Vavilov generator is beneficial, but whether the 5 % improvement is worth the computational overhead, is debateable considering that the intrinsic accuracy of the distribution is thought to be poorer.

Transitions between the distributions

The transitions between the Landau and Vavilov distribution is shown on the left in Fig. 1.4 for $\kappa = 0.21$. For lower values of κ , the Landau and Vavilov distributions are barely distinguishable. The transition point in Garfield is at $\kappa = 0.05$. The transition between the Vavilov and Gaussian distribution is shown on the right for $\kappa = 1.3$, which is well below the transition point in Garfield at $\kappa = 5$.

Comparison with Heed

As shown in Fig. 1.6, the energy loss distribution computed with the Heed program, agrees with the model described above. Agreement is poorest for the thinnest layers, where the Landau distribution is supposed to be applicable. The Heed program has been extensively tested for energy loss by GeV-energy charged particles traversing gas detectors.

1.4.7 Convolution properties

Since we wish to generate energy deposition patterns, with spatial detail, we will need to subdivide the layer and deposit energy in each of these. For this to be a consistent approach, we need to ascertain that the distributions f of the energy loss ϵ satisfy to a sufficient precision the convolution property:

$$f(\epsilon|nd) = f(\epsilon|d)^{*n}$$

where “*” stands for multiple convolution.

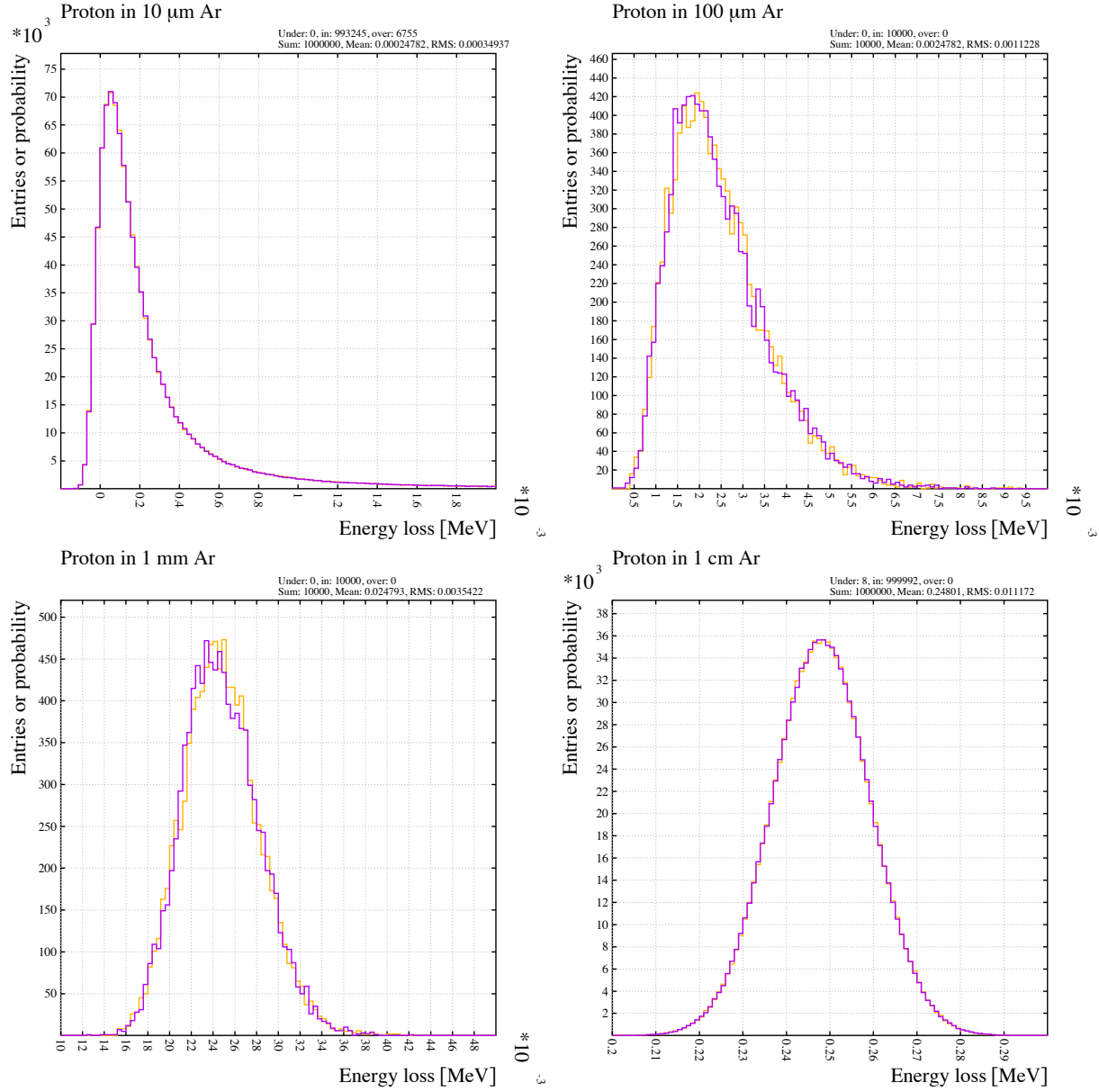


Figure 1.7: The distribution of the energy deposited by a proton with a kinetic energy of $E_{\text{kin}} = 1$ MeV in a single layer (orange) of argon of thickness 10 μm , 100 μm , 1 mm and 1 cm should be the same as the energy deposited in 5 successive layers of 1/5th the thickness (purple).

The mean energy loss $\bar{\epsilon}$ and the energy loss parameter ξ both scale linearly in d . The maximum energy transfer E_{max} does not depend on d . As a result, the multiple-thickness sampling parameter $\lambda_{nd}(\epsilon)$ as used with the Landau and Vavilov distributions, is related to the single-thickness parameter $\lambda_d(\epsilon)$ by:

$$\lambda_{nd}(\epsilon) = \frac{1}{n} \lambda_d(\epsilon) - \log n$$

This precisely matches the convolution property of the Landau distribution

$$f_L(\lambda) = n f_L(n\lambda + \log n)^{*n}.$$

Thus, the convolution property holds exactly for the complete Landau distribution. We however use a truncated Landau distribution, for which the convolution property is not satisfied exactly. In particular, there will be distortions in the high-energy part of the distribution.

Presumably, the Vavilov distribution satisfies similar convolution properties as the Landau distribution (to be verified).

The convolution property for the Gaussian distribution is trivially satisfied since σ^2 and $\bar{\epsilon}$ both are proportional to d .

The above properties are, as shown in Fig. 1.7, satisfied by the combined generator.

1.5 Ionisation electron statistics

The Heed program itself converts electromagnetic energy losses into ionisation electrons. The SRIM output doesn't contain information on this process. Given that the Heed model closely reproduces the experimental data available, Garfield applies the Heed model for this conversion also to SRIM generated ionisation patterns.

In the Heed model, the electromagnetic energy loss is transformed into ionisation electrons in an iterative process:

- the electromagnetic energy loss δE for a step is computed;
- to the energy loss δE is added the unused electromagnetic energy loss E_{rest} from earlier steps, if any;
- single-electron formation energies are drawn from a custom-designed distribution, and subtracted from δE , as long as δE remains positive;
- the energy that remains is assigned to E_{rest} for use in a following step, if any.

The distribution of single-electron formation energies is designed to be such that the above process, for high electromagnetic energy losses, produces the work function and Fano factor appropriate for the gas. The distribution is generated from a reference distribution which is flat for $w/2 < E < w$, falling as $(w/E)^4$ for $w < E < 3.064w$, and zero outside these limits. This reference distribution leads to a Fano factor of 0.174. Distributions for other work functions and Fano factors are obtained by scaling the reference distribution, as explained in [Igor Smirnov, NIM A 554 (2005) 474].

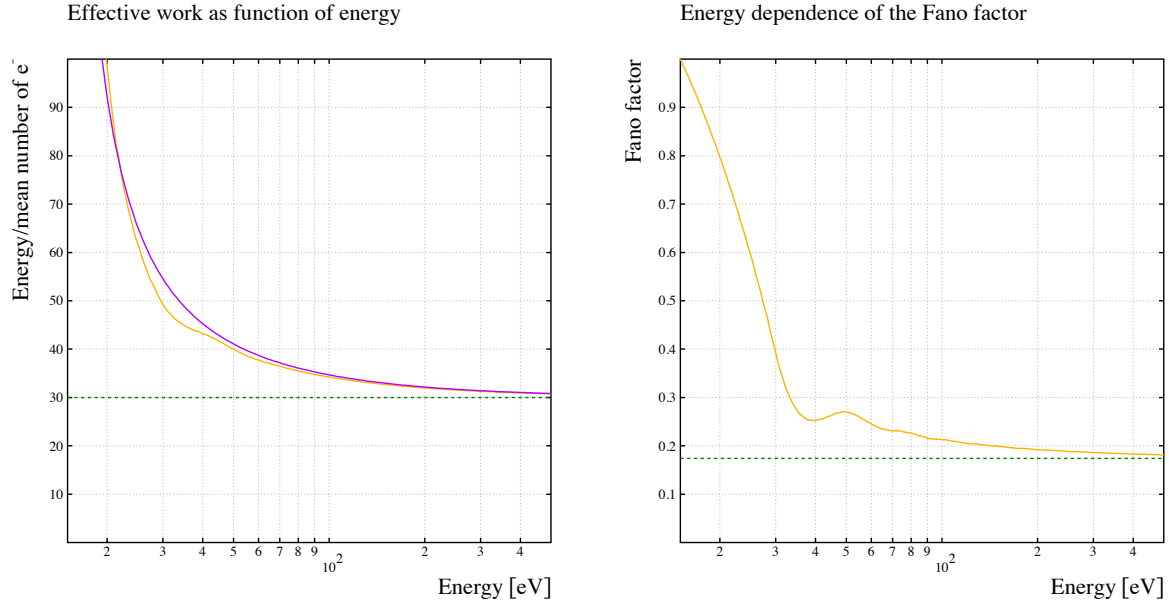


Figure 1.8: The effective work at low electromagnetic energy loss is considerably larger than the nominal work (orange line). This effect is well reproduced by the phenomenological model shown in purple. Similarly, the Fano factor at low energy loss is close to 1 and it reaches its asymptotic value only well above the nominal work function. This is illustrated here for a gas with work function $w = 30\text{eV}$ and Fano factor $F = 0.174$.

The work function of a gas is, as a rule, roughly twice the ionisation energy. The Fano factor seems to be correlated with the ionisation factor as reported for instance in [A. Pansky, A. Breskin and R. Chechik, J. Appl. Phys. 82 (1997) 871]. Both the work function and the Fano factor have, in addition, a dependence on the electromagnetic energy as illustrated in Fig. 1.8.